Chapter VIII

Adsorption Studies using Nano/ Magnetic Nanocomposites

The rapid development of nanotechnology has aroused great interest in environmental remediation. Several research studies are being carried out using nanomaterials in the removal of toxic metal species from polluted waters. In this scenario, the present chapter deals with the preparation of nanosized materials of TPJB/ TGH precursors and their corresponding nanocomposites employing Fe_3O_4 as dopant, which exhibit magnetic characteristics. Batch mode results revealed TPJB and TGH to show better sorption characteristics in preference to TTIH. In this context, the experimental set-up were restricted with TPJB and TGH.

8.1 Preparation of Nanomaterials

TPJB and TGH were subjected to milling process [Planetary Ball Miller (***Model- VBCC/PM/24-13/14***)]. 20 grams of each were ground in a jar at 260 revolutions/ minute along with tungsten carbide balls for 3/ 10 hours respectively. The resulting nanosized materials are thereafter referred to as NTPJB and NTGH. Figure 8.1 and 8.2 denote the Planetary ball miller instrument and grinding set-up.

Figure 8.1 Planetary Ball Miller

Figure 8.2 Jar with Sorbent and Tungsten Carbide Balls

8.1.1 Atomic Force Microscopic Analysis

A three dimensions view of NTPJB and NTGH, their corresponding microscopic histograms are depicted in figures 8.3 – 8.6. Appearance of marked peaks around 9 nm and 35 nm imply the existence of nanosized NTPJB and NTGH.

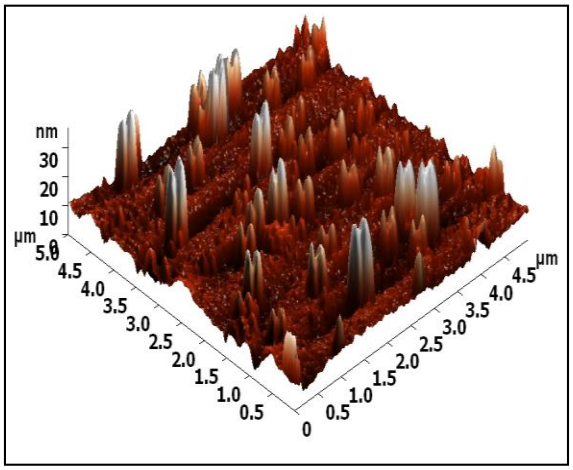

Figure 8.3 3-D Surface Topography of NTPJB

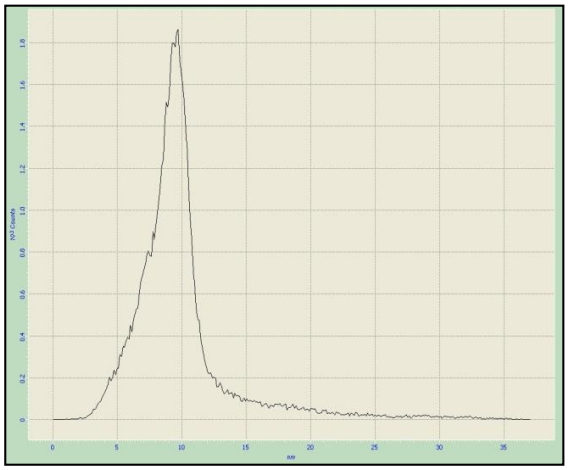

Figure 8.4 Histogram of NTPJB

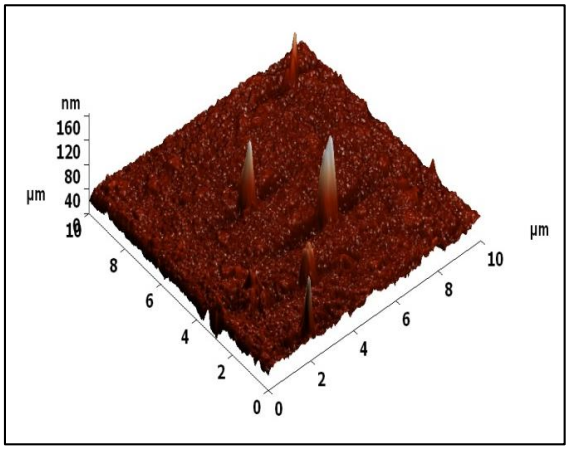

Figure 8.5 3-D Surface Topography of TGH

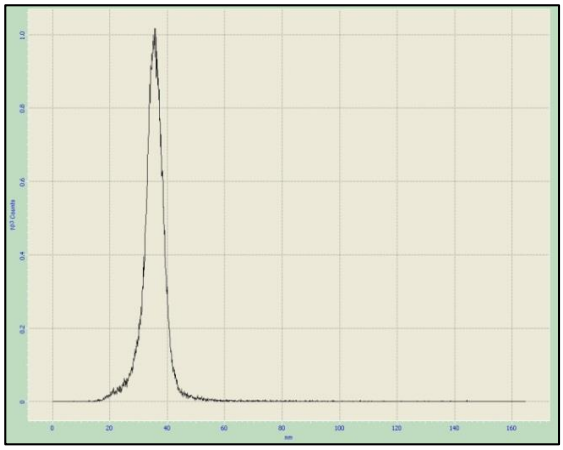

Figure 8.6 Histogram of NTGH

8.2 TG/ DTA Analyses

TG/ DTA analyses of the synthesized NTGH using DTG-60 (Shimadzu- Japan) instrument were carried out to determine its thermal stability. TG/ DTA curves were recorded under an O_2 atmosphere at a flow/ heating rates of 4 mL/ min and 20°C/min (Figure 8.7). The initial weight loss upto 250°C may be due to the loss of water molecules bound to keratin present in the goat hoofs. Further, loss between 250°C and 550°C shown as steep reduction in the curves can be ascribed to the degradation of amine group[171]. Beyond 550°C, appreciable weight loss is not observed. It is understood that these analyses exhibit the presence of keratin material along with organic and mineral composites[172].

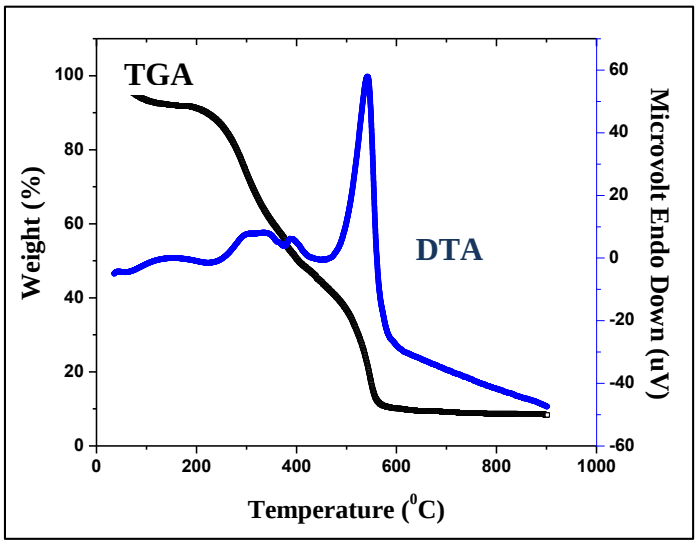

Figure 8.7 TG / DTA Curve – NTGH

8.3 Batch Experiments using NTPJB and NTGH

Pb(II), Cd(II), Ni(II) solutions with an initial concentration of 100 mg/ L were agitated with different doses (50 - 200 mg: 50 mg) of synthesized nanomaterials at a predetermined time frames of 30 min (NTPJB) and 5 min (Pb(II) – NTGH), 10 min (Cd(II) – NTGH) and 20 min (Ni(II) – NTGH), respectively. The results indicate that maximum removal of chosen ions had occurred at 150 mg/ 100 mg against 300 mg required for TPJB and 200 mg in case of TGH (Table 8.1).

The same doses of NTPJB (150 mg) and NTGH (100 mg) has been required for maximum removal of Pb(II) [83.4 mg/L] from effluent and Cd(II)/ Ni(II) [100 mg/L] synthetic solutions, wherein the removal percentage are found to be lesser than corresponding aqueous solutions, which intend to the occurrence of interfering ions in the case of former (Table 8.2).

Table 8.1 Effect of NTPJB/ NTGH on Aqueous Solutions

Weight of Adsorbent (mg)	Percentage Removal (%)					
	NTPJB			NTGH		
	Pb(II)	Cd(II)	Ni(II)	Pb(II)	Cd(II)	Ni(II)
50	79.4	77.6	73.4	90.3	87.6	82.9
100	83.6	80.1	73.8	**95.2**	**94.7**	**88.2**
150	**89.3**	**88.2**	**76.7**	93.5	91.9	86.5
200	87.5	84.6	75.9	92.2	91.4	86.1

Table 8.2 Effect of NTPJB/ NTGH on Effluent and Synthetic Solutions

Adsorbents	Weight of Adsorbents (mg)	Percentage Removal (%)		
		Effluent	Synthetic Solutions	
		Pb(II)	Cd(II)	Ni(II)
NTPJB	50	66.8	69.2	63.5
	100	69.3	69.4	65.4
	150	**72.3**	**70.5**	**69.2**
	200	70.2	68.6	67.9
NTGH	50	84.8	80.4	79.6
	100	**87.2**	**83.1**	**80.3**
	150	85.6	80.5	78.8
	200	84.7	79.2	76.2

As an outcome of NTJB and NTGH results, TGH registered better chelating ability for magnestization studies. Therefore, TGH samples was magnetized using the following procedures.

8.4 Synthesis of Magnetic Nanocomposites

8.4.1 Preparation of Fe_3O_4 from Ferric Chloride

0.1M Ferric chloride and 0.4 M Potassium iodide solutions were prepared from which 150 mL and 50 mL each were mixed and stirred for one hour at room temperature to facilitate the precipitate. Later, the formed precipitate was filtered, washed thoroughly with doubly distilled water and dried in a hot air oven (100°C). The material was hydrolyzed through dropwise addition of 25% ammonia solution along with continuous stirring to ensure the black magnetite (Fe_3O_4) precipitate. The entire procedure was carried out in a basic pH environment (pH 9-11)[173]. This black precipitate was filtered/ washed/ dried at 250°C and stored. TGH and the dried powder were thoroughly mixed in 1:1 ratio and referred to as TGH-C1, prepared through ex-situ formation. Schematic representation of the above procedure is shown below.

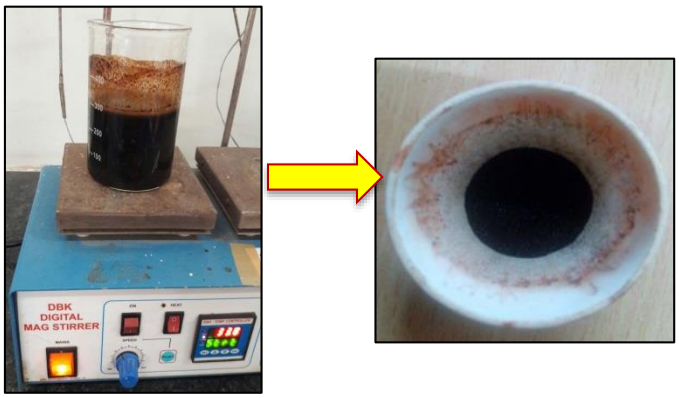

8.4.2 Preparation of Fe_3O_4 using Ferric Benzoate

80 mL of 0.4 M Ferric nitate solution was added to 150 mL of 0.4 M benzoic acid resulting in the precipitation of ferric benzoate, after continuously stirring for 20 mins in a magnetic stirrer. The yellow coloured ferric benzoate was filtered, later washed with hot distilled water and dried. 8 g of ferric benzoate was added to the 50 mL of doubly distilled water along with 10 g of TGH. The mixture was stirred for 6 hours, the obtained solid was filtered, dried and heated in a muffle furnace (600°C) for 10 minutes, resulting in the formation of TGH - Fe_3O_4 nano composites[174] through one –pot synthesis, thenceforth called as TGH-C2.

8.4.3 Preparation of Fe_2CrO_4 using Iron/ Chromium Salts

50 mL each of the nitrate solutions corresponding to iron (2 M) and chromium (1 M) were taken in a beaker, to which 28 % urea solution was added. The mixture underwent combustion, later heated/ stirred on a magnetic hot plate. TGH was added to the prepared Fe_2CrO_4 precipitate and heated in a muffle furnace for 2 hours[175]. The dried lumps obtained were ground well, stored and denoted as TGH-C3. The photographs of auto combustion process and the magnetic property of TGH – C3 are shown below.

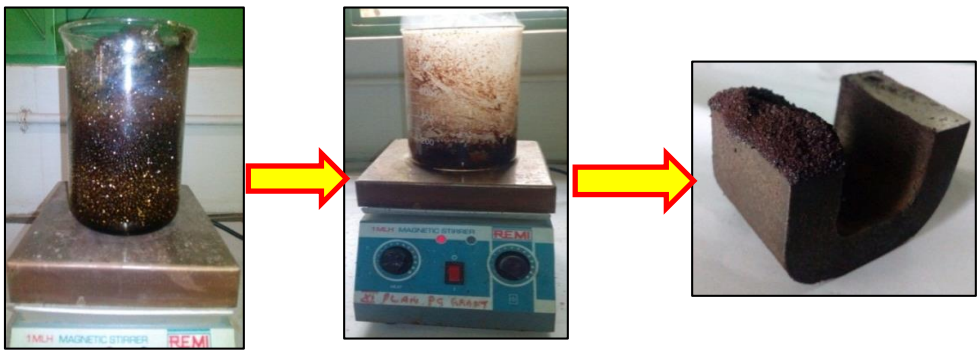

The prepared nanocomposites were found to possess magnetic nature which are depicted as follows.

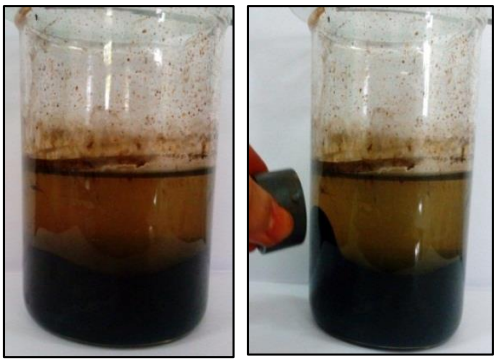

TGH- Fe_3O_4 – Ex-situ Synthesis

TGH- Fe_3O_4 – One Pot Synthesis

8.5 Characterization of TGH – C1, C2 and C3

8.5.1 VSM Analysis

The characteristic magnetic features of TGH – C1, C2 and C3 were established using a Vibrating Sample Magnetometer (VSM) and the resulting hysteresis loops are depicted in figure 8.8. These loops reveal the paramagnetic behavior of the composites. Saturation magnetization (M_s), coercivity (H_{ci}) and retentivity (M_r) values derived as per specifications of the loops are tabulated in 8.3.

Table 8.3 VSM Measurements

MNC's	Saturation Magnetization (M_s) emu/g	Coercivity (H_{ci})G	Retentivity (M_r) emu/g
TGH – C1	18.85	54.62	0.78
TGH – C2	3.90	95.53	0.27
TGH – C3	3.08	154.55	0.34

The M_s values for TGH- C1 is found to be greater than C2 and C3 samples, indicative of low attainment of saturation in the latter. This is supported by the greater H_{ci} value of TGH- C3 in favour of the inverse relation between the M_s and H_{ci} values[176]. The low retentivity (M_r) values imply lesser residual magnetism levels, invariably for all the samples as their less than unity.

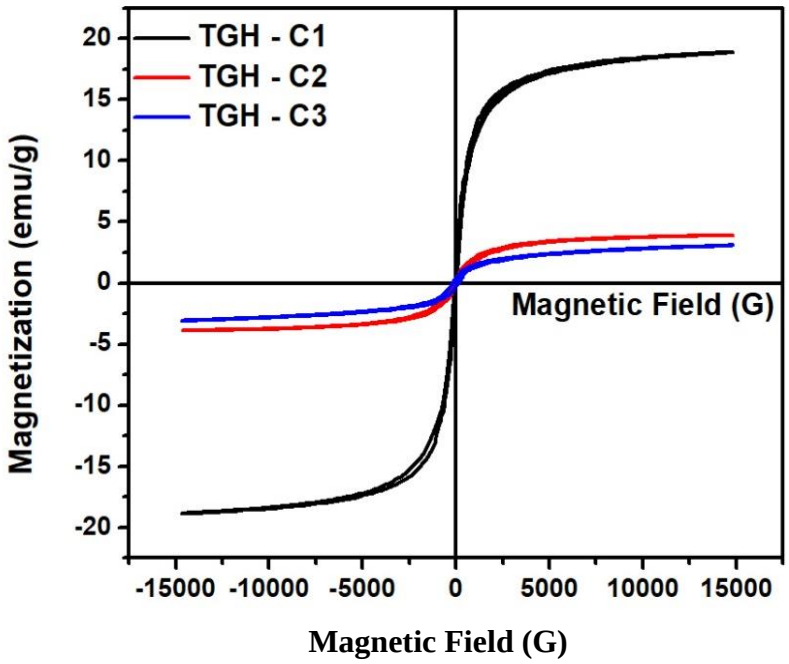

Magnetic Field (G)

Figure 8.8 VSM Analysis of Magnetic Nanocomposites

8.5.2 XRD Analysis

The prepared composites were subjected to X-ray Diffraction analysis and the obtained patterns are shown in figure 8.9. The amorphous nature of TGH is favoured by the broad peak at 20.34° corresponding to the presence of keratin group in TGH[177] and certain crystalline peaks at 37.25°, 46.55° refer to Ca group and 66.76°/ 79.22° are indicating the presence of Si and CaO[178] respectively.

The main characteristic peaks of TGH – C1, C2 with the lattice value of (220), (311), (400), (511) and (440) relate to the Fe_3O_4 phase[173, 174]. The sites and intensity of the diffraction peaks in C1 and C2 stand consistent with the regular pattern of Magnetite (Fe_3O_4) through the JCPDS Card No. (89 - 0691). XRD spectrum of TGH-C3 exhibits typical peaks at 30.1º, 35.5º 43.15º, 57.07º and 62.67º are indexed as (220), (311), (400), (511) and (440) being reliable on the standard pattern of iron chromium oxide[175] for JCPDS Card No. (89 - 2618). As per figure 8.9, TGH – C2 composite recorded an X-ray pattern with diminished height than the other two composites. The reason could be the utilization of organic reducing agent (benzoic acid) which depress the iron oxide nanoparticles in the mixture and affects further interaction.

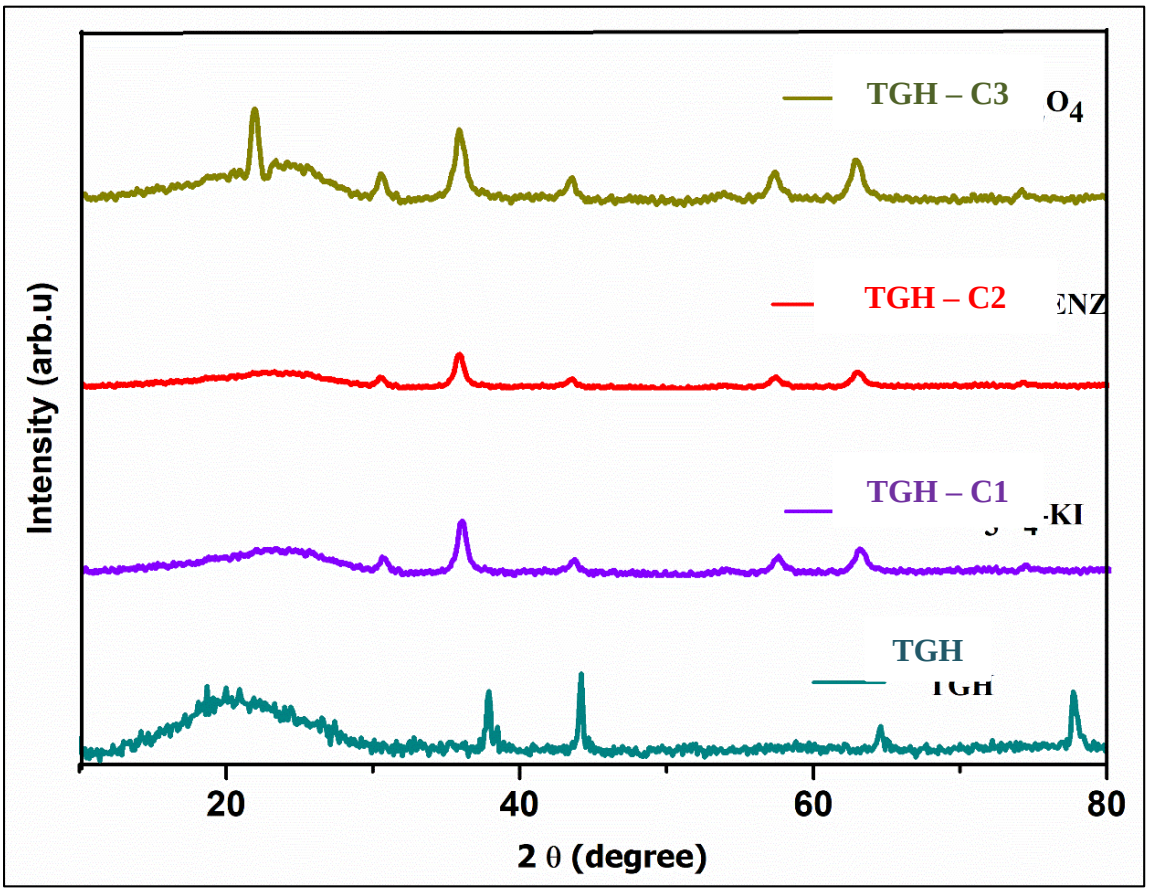

Figure 8.9 XRD Spectra of Magnetic Nanocomposites

8.5.3 SEM/ EDAX Analyses

SEM images of synthesized TGH– C1, C2 and C3 represented in figures 8.10 - 8.12 exhibit the presence of small aggregate particles of uneven sizes. EDAX spectra of iron oxide embedded TGH (Figures 8.13 - 8.15) describe the presence of K, Cl, Cr, Fe and O elements, where the calculated atomic ratio of Fe and O is 3:4, confirming the formation of magnetite (Fe_3O_4) in the composites.

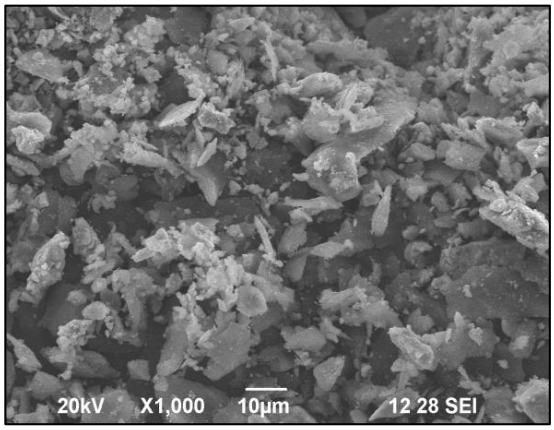

Figure 8.10 SEM: TGH – C1

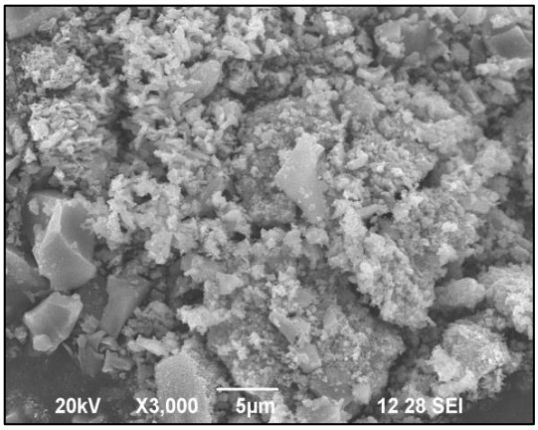

Figure 8.11 SEM: TGH – C2

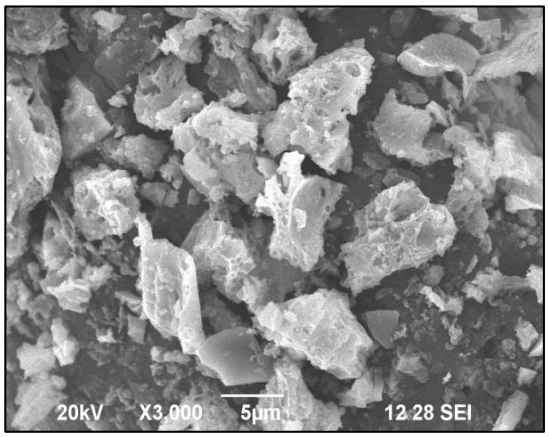

Figure 8.12 SEM: TGH – C3

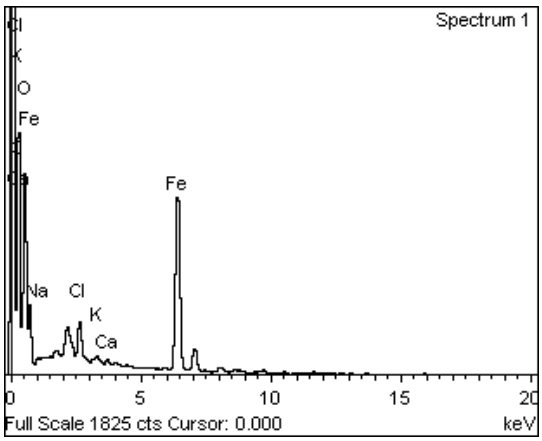

Figure 8.13 EDAX: TGH– C1

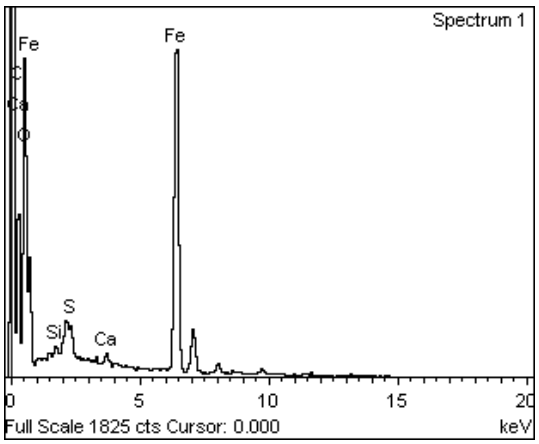

Figure 8.14 EDAX: TGH –C2

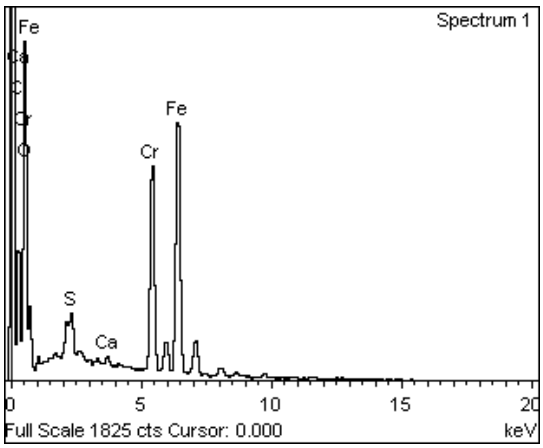

Figure 8.15 EDAX: TGH –C3

8.5.4 FTIR Spectral Studies

Figure 8.16 depicts the FT-IR spectra of TGH and its respective composites, where (b), (c) and (d) exhibit specific peaks at 640.39, 566.13and 583.49 cm^{-1} along with the prominent peaks corresponding to several functional groups (a), as illustrated in 6.4. It is clear from this statement that, the core structure of TGH is not disturbed during precipitation process[179] as the characteristics peaks are retained. Also, the strong new peaks referred to the binding of Fe–O group to the TGH matrix, sufficing the magnetic characteristics of the composites[180, 181, 182].

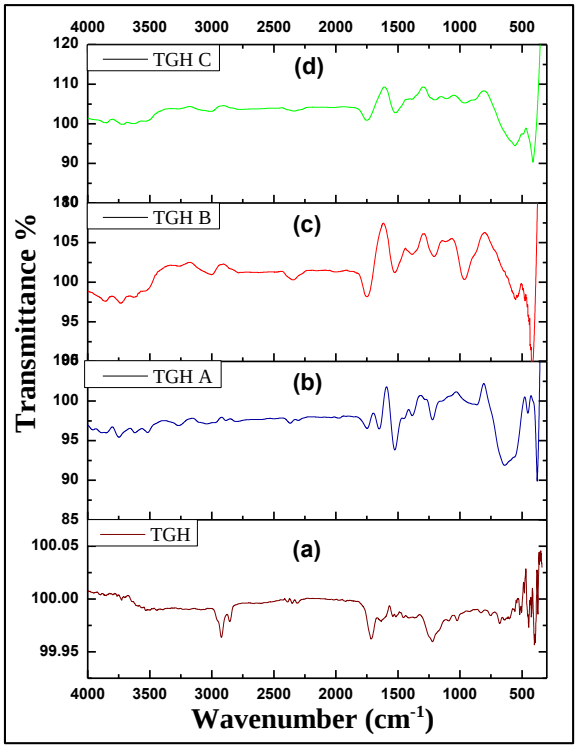

Figure 8.16 FTIR Spectra of TGH and Magnetic Nanocomposites

8.6 Batch Studies using TGH – C1, C2 and C3

The sorption characteristics of synthesized nanocomposites were verified through pilot studies and later extended to field samples/ synthetic solutions. Varied doses (25 mg – 100 mg: 25 mg) were added to the respective solution and agitated under optimized conditions. The results are graphically represented in figures 8.17 and 8.18, where 50 mg and 75 mg each of TGH – C1, C2 and C3 were sufficient for the maximum percentage removal (Tables 8.4 and 8.5).

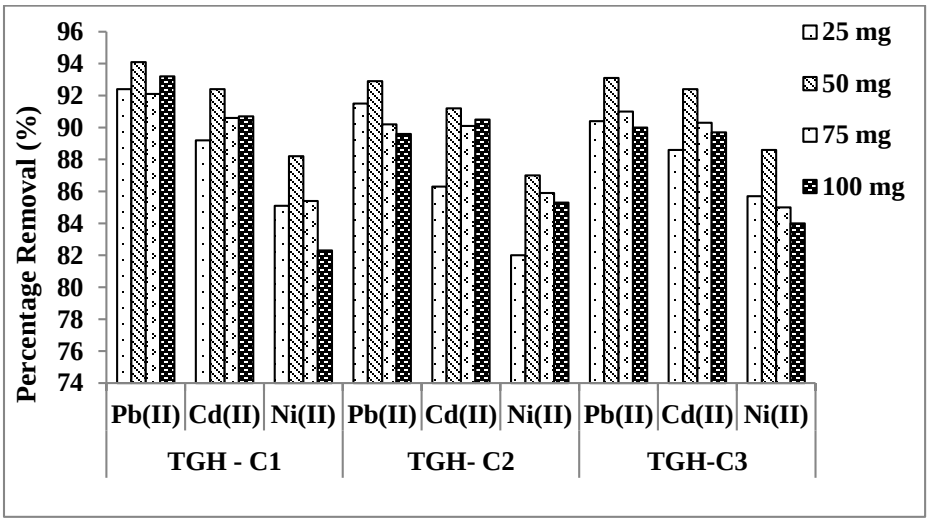

Figure 8.17 Effect of Dosage – Aqueous Solutions

Table 8.4 Effect of Magnetic Nanocomposites – Aqueous Solutions

Weight of Composites (mg)	Percentage Removal (%)								
	TGH - C1			TGH- C2			TGH-C3		
	Pb(II)	Cd(II)	Ni(II)	Pb(II)	Cd(II)	Ni(II)	Pb(II)	Cd(II)	Ni(II)
25	92.4	89.2	85.1	91.5	86.3	82.1	90.4	88.6	85.7
50	**94.1**	**92.4**	**88.2**	**92.9**	**91.2**	**87.2**	**93.1**	**92.4**	**88.6**
75	92.1	90.6	85.4	90.2	90.1	85.9	91.4	90.3	85.5
100	93.2	90.7	82.3	89.6	90.5	85.3	90.2	89.7	84.8

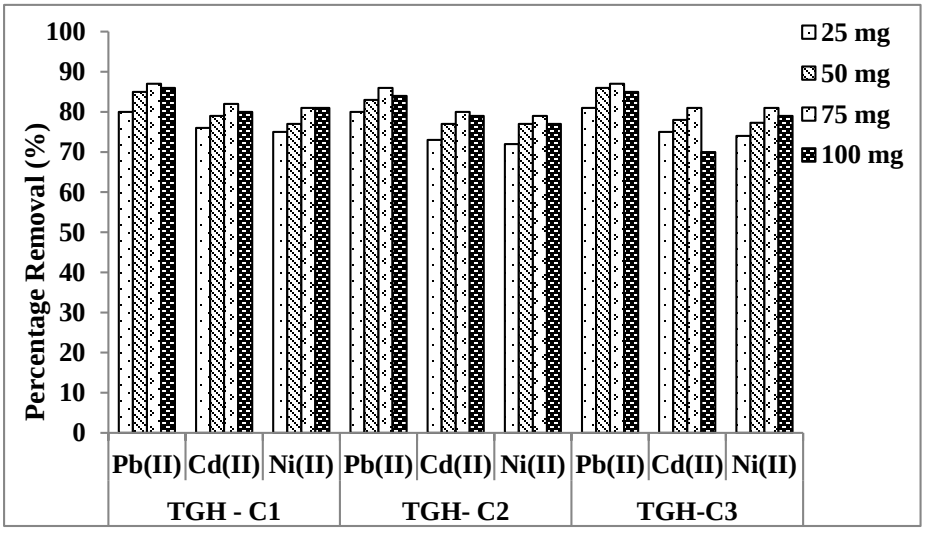

Figure 8.18 Effect of Dosage – Effluent/ Synthetic Solutions

Table 8.5 Effect of Magnetic Nanocomposites – Effluent/ Synthetic Solutions

Weight of Composites (mg)	Percentage Removal (%)								
	TGH - C1			TGH- C2			TGH-C3		
	Pb(II)	Cd(II)	Ni(II)	Pb(II)	Cd(II)	Ni(II)	Pb(II)	Cd(II)	Ni(II)
25	80.2	76.3	75.6	80.4	73.1	72.8	81.5	75.4	74.2
50	85.3	79.5	77.2	83.8	77.1	77.4	86.2	78.4	77.3
75	**87.5**	**82.1**	**81.8**	**86.7**	**77.9**	**79.1**	**87.3**	**81.1**	**81.4**
100	86.1	80.4	81.2	84	76.7	77.3	85.6	70.2	79.6

The better metal chelating property of TGH-C1 is confirmed by Zeta potential and Particle size analyses. Zeta potential analysis has been accomplished to confirm the surface charges of the composites. The Z_{PC} values for TGH-C1, C2 and C3 were measured using ZPC analyzer and observed to be negative (-0.154, -0.124 and -0.997 mV). These negative surface charge values promote enhanced sorption of positively charged metal ions, wherein TGH – C1 sample registered more negative value, favouring better metal sorbing ability.

The Dynamic Light Scattering method was used to analyze the average particle sizes of composite in liquid phase. The results show the sizes of TGH-C1, C2 and C3 to be 91.28 nm, 173.1 nm and 163.9 nm respectively (Figures 8.19 – 8.21). TGH – C1 has the smaller nm parametric value than C2 and C3 samples, supporting the tabulated batch values.

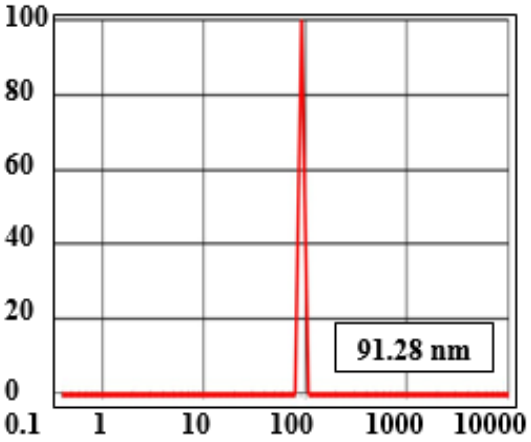

Figure 8.19 Particle Size – TGH – C1

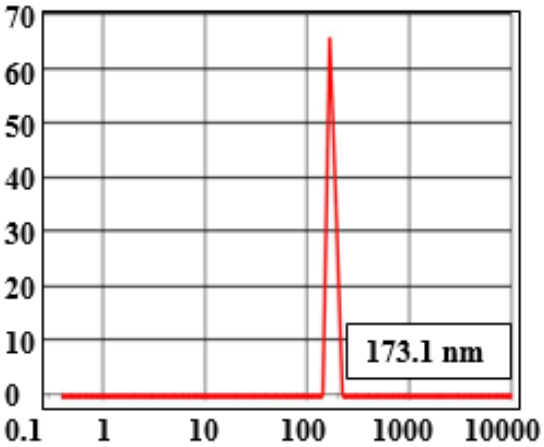

Figure 8.20 Particle Size – TGH – C2

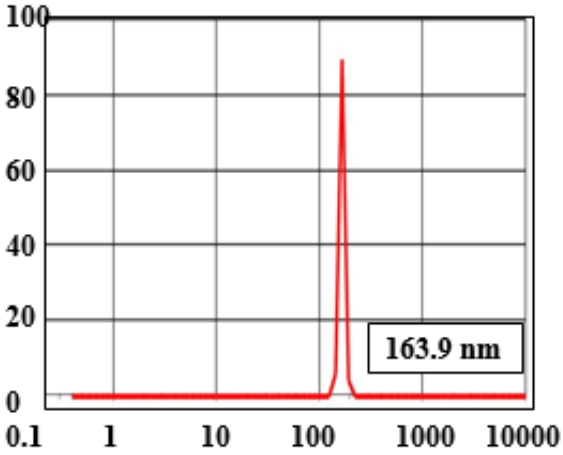

Figure 8.21 Particle Size – TGH – C3